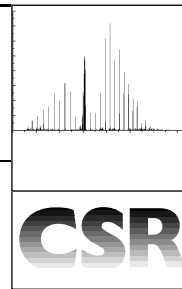


# Near-infrared diode laser spectroscopy in chemical process and environmental air monitoring



Philip A. Martin

Department of Chemical and Biological Sciences, University of Huddersfield, Queensgate, Huddersfield, UK HD1 3DH. E-mail: p.a.martin@hud.ac.uk; Fax: +44 (0)1484 472182; Tel: +44 (0)1484 473345

Received 22nd November 2001

First published as an Advance Article on the web 21st June 2002

This review covers the rapidly expanding field of near-infrared tunable diode laser spectroscopy where the availability of new lasers has led to the development of simple and inexpensive spectroscopic systems for the detection and monitoring of gas species. The latest diode lasers and the specific techniques associated with diode laser spectroscopy are described. Specific examples covering chemical vapour deposition reaction diagnostics, remote vehicle emission sensing, balloon-borne atmospheric monitoring and combustion diagnostics then illustrate the technique advantages of rapid, highly selective, *in situ* monitoring.

## 1 Introduction

Until the end of the 1980's IR laser absorption spectroscopy had been mainly restricted to research laboratory experiments in fundamental spectroscopy and kinetics but since then there has been a rapid expansion towards its use in more applied areas such as in atmospheric and pollution monitoring as well as process monitoring and control in industrial environments. These advances have been primarily led by improvements in laser technology and associated electro-optics deriving from expanded applications in the telecommunications and consumer electronics industries.

In addition to this there has been an increased interest in direct measurement in the atmosphere and in the environment in

general. In parallel, the drivers are for improving process efficiencies by understanding the chemistry and physics of the process and by requirements for *in situ* monitoring instead of extractive, batch sampling. This article attempts to review this exciting and rapidly developing area of chemistry where *in situ* measurements can now be made rapidly with unprecedented sensitivity, accuracy and precision.

Traditionally diode lasers based on lead salts or alloys have been the principal tunable laser source in the infrared, both for high sensitivity trace gas detection and for the determination of molecular line parameters, often employing long path absorption cells at low pressure. Detection limits in the parts per billion range are routinely achieved by detecting strong molecular vibrational transitions in the mid-infrared (defined here as 3–30  $\mu\text{m}$ ). Such high sensitivities enable rapid, time-evolving systems to be studied and in an *in situ* and non-invasive manner. High species specificity is derived from the very narrow wavelength spread of the laser emission. In an absorption experiment the narrow laser emission is wavelength tuned through a much broader molecular absorption and the change in detected laser power is measured. For many applications, however, lead-salt diode laser spectrometers are limited by the requirement for cryogenic cooling of the lasers and detectors as well as the low output emission power in the  $\mu\text{W}$  range which is often spread over several discrete wavelengths (multimode emission). In many ways, lead-salt diode lasers have failed to meet initial expectations for widespread use and laser device developments have thus been limited by the lack of other consumer or telecommunication applications. Much of the lead-salt diode laser spectroscopy field has been reviewed previously.<sup>1,2</sup>

In contrast, enormous investment from the telecommunications industry has led to much greater advances being made in diode lasers made from elements of Groups III and V such as gallium and arsenic for operation in the near-infrared (NIR, defined here as 0.8–3  $\mu\text{m}$ ). Unfortunately for spectroscopic purposes, operating in the near-infrared decreases the detection sensitivity because weaker vibrational transitions are being detected (vibrational overtone and combination bands). However, this is outweighed in many cases by the tremendous practical advantages of easy to use, robust, reliable devices operating at room temperature with relatively high output emission power (mW) and at single discrete wavelengths (single mode). In addition, they can be used with fibre optic technology and inexpensive spectrometer components. The technical advantages still remain of a very narrow wavelength spread of the light emission so that interferences from other transitions are negligible (high molecular specificity) and the ability to directly vary the output emission (modulate) to improve detection sensitivities (see later).

These advantages open up a wide range of new applications taking high resolution laser spectroscopy out of the research

Philip A. Martin completed his BA in Chemistry at the University of Oxford in 1985 and then moved to the University of Cambridge in the group of Dr Paul Davies to study the IR laser spectroscopy of transient species. After completing his PhD in 1989 he received a Royal Society European Exchange Fellowship to work at the Université de Paris-Sud in the group of Guy Guelachvili on molecule selective techniques in high resolution FTIR. He later spent 3 years in the group of Professor John Maier at the University of Basel, Switzerland and is now a Reader at the University of Huddersfield, UK. Research interests are gas phase spectroscopy, laser spectroscopy, air pollution, process control and he has recently set up a spin-off company, TDL Sensors Ltd.



laboratory and into industrial locations or into the atmospheric environment. Recent applications have covered *in situ* atmospheric sensing, gas flux measurement by eddy correlation, plasma and combustion diagnostics, remote car exhaust monitoring, medical applications such as breath analysis, quality control of high purity gases and explosives measurements. NIR diode laser spectroscopy meets the requirements of industrial sensors for process control and stack emissions especially in high temperature environments up to 1500 °C for species such as O<sub>2</sub>, H<sub>2</sub>O, HCl, NH<sub>3</sub>, CO, CO<sub>2</sub> with accurate and precise measurements in the presence of other gases and high dust loads. The technique allows continuous measurements with rapid response times. For process monitoring and control in the manufacturing sector this can lead to increased efficiencies and reduced development times for new products. Additionally there are safety advantages in non-invasive sampling and the use of fibre optic light transmission so that the monitoring and control equipment can be kept at a safe location.

For many of the applications mentioned above the only alternatives have been non-optical methods such as mass spectroscopy or gas chromatography both of which require extraction and preconditioning of samples. Direct physical contact between the gas sample and the sensor can also lead to slow response times, hysteresis effects due to irreversible contamination, limited selectivity and drifting backgrounds. Optical methods only require direct optical access with no sample preparation. Instruments based on broad-band IR sources such as FTIR, FTNIR spectrometers as well as wavelength dispersive instruments in the NIR have the main advantage of wide spectral coverage and are ideal for multi-component analyses of complex mixtures of unknown gases but lack sensitivity and specificity and can be considered to be complementary to diode laser methods. Differential optical absorption spectroscopy or DOAS and LIDAR (light detection and ranging) often require complex chemometrics to extract information.<sup>3,4</sup>

It must be mentioned that there are several disadvantages of near-infrared diode laser absorption spectroscopy. Each laser only wavelength tunes over a narrow range, effectively limiting each laser to single species measurement. However this can be overcome either by using external cavity diode lasers (ECDL) which can give wider wavelength tuning ranges or by combining laser light (wavelength multiplexing) using standard telecommunications equipment so that multicomponent analysis is possible. Availability of the lasers at wavelengths outside the telecommunication regions can still be problematical.

The review focuses on advances over the past five years or so as other reviews have covered the near-infrared diode laser spectroscopy field up to this point.<sup>5,6</sup> Although the study of fundamental vibrational transitions with mid-infrared lasers has continued, many of the important advances have now come from the development of near-infrared laser technology (for the telecommunications industry). The review focuses mainly on chemical applications rather than the technology, although recent advances in laser sources and specific techniques related to IR laser spectroscopy such as harmonic detection and cavity ring-down spectroscopy are described as well as the types of spectroscopic information that can be obtained in the near-infrared. Several diverse applications are then discussed in more detail to illustrate the capabilities. Finally, the future prospects and developments are considered.

## 2 Diode laser sources for spectroscopy

It is not the purpose of this review to discuss the details of laser structure and operation as these can be found in other reviews,<sup>7,8</sup> but it is beneficial to describe the basic types and their properties.

A semiconductor diode laser consists of a junction between a p-type semiconductor and an n-type semiconductor. When an electric current flows across the junction, electrons and holes can recombine, emitting light in the process. The emission wavelength is determined by the band gap of the semiconductor material making up the diode. Pure gallium arsenide (GaAs), for example, has an emission wavelength of 904 nm but can be doped to produce different band gaps and thus wavelengths. InGaAsP/InP devices are used for optical communications and have been developed primarily around 1330 and 1550 nm but can be manufactured to cover the range 1100–1800 nm where many gases have vibrational transitions. For longer wavelengths, antimonide compounds have been developed such as AlGaAsSb and InGaAsSb with room temperature continuous wavelength operation.<sup>9</sup> Towards longer wavelengths room temperature operation becomes more difficult due to the increased optical and electrical losses. Lead-salt diode lasers have undergone a much lower level of development than the GaAs-based diode lasers and still require cryogenic cooling for continuous operation. They are still being developed by Tacke and coworkers.<sup>10</sup> In simple devices, the wavelength is tuned by varying the temperature of the laser (slow tuning) or by varying the electric current (fast tuning). The lasers are manufactured by both molecular beam epitaxy and metal-organic chemical vapour deposition.

For spectroscopic applications, the main requirements are single mode emission and this has been achieved by employing wavelength-selective elements such as gratings into the laser cavity, either directly into the diode substrate by holographic printing in the active area as in the distributed feedback (DFB) laser (Fig. 1a) or external to the diode as in the external cavity diode laser (ECDL) (Fig. 1b). In the ECDL, single mode operation can be possible over more than 100 nm compared to

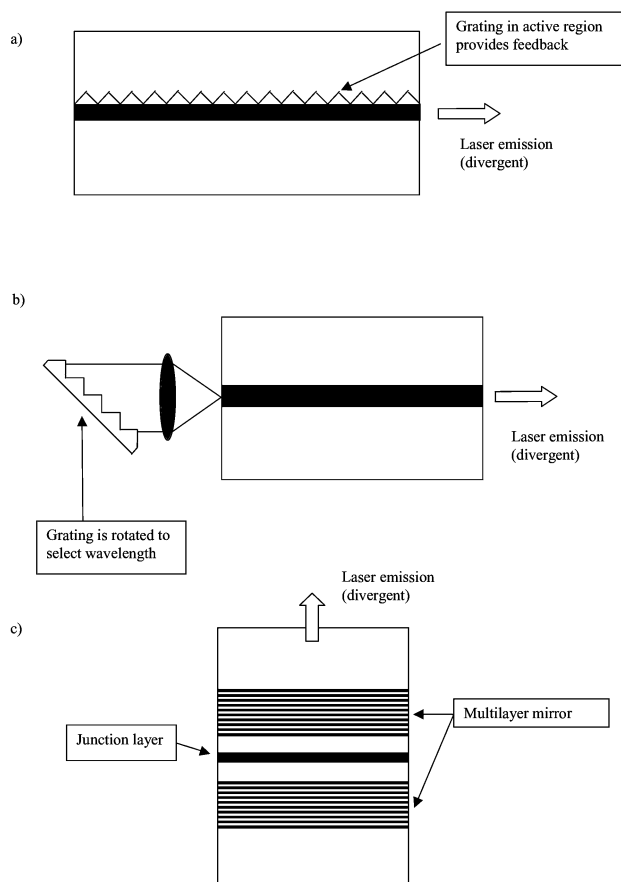


**Fig. 1** Schematic drawings of (a) a distributed feedback (DFB) diode laser, (b) an external cavity diode laser, and (c) a vertical cavity surface emitting laser (VCSEL).

2–3 nm for the DFB laser. Typical single mode output powers for DFB lasers and ECDL are in the milliwatt range with room temperature operation.

Vertical cavity surface emitting lasers (VCSEL) (Fig. 1c) emit light from the surface rather than the end facet. The cavity mirrors, which are stacks of thin layers of alternative refractive indices, are placed above and below the junction layer. VCSELs produce circular beams, have lower threshold currents and are more efficient but are so far limited to shorter wavelengths. They have been successfully used for oxygen sensing around 760 nm.<sup>11</sup>

One of the more recent developments is the quantum cascade laser.<sup>12,13</sup> Strictly speaking they are not diode lasers as the emitted wavelength depends on the thickness of the semiconductor layers rather than the band gap. Electrons cascade down a set of energy drops emitting light in the mid-IR range. At the current stage of development near room temperature operation is possible only in pulsed mode operation.

### 3 Diode laser spectroscopy techniques

Although diode laser spectroscopy is based on standard absorption spectroscopy several different detection techniques have been developed to enhance sensitivity and it is instructive to consider some of these.

#### Absorption spectroscopy

Diode laser spectroscopy is an absorption technique and is thus governed by the Beer-Lambert law, with the transmitted laser intensity:

$$I(\nu) = I_0(\nu)\exp(-\sigma(\nu).N.L) \quad (1)$$

where  $I_0(\nu)$  is the transmitted intensity in the absence of absorbing species,  $L$  is the absorption pathlength in cm,  $N$  is the concentration of absorbing species in molecules  $\text{cm}^{-3}$  and  $\sigma(\nu)$  is the absorption cross-section in  $\text{cm}^2$  molecules $^{-1}$ . The absorption coefficient,  $\alpha(\nu)$ , is given by

$$\alpha(\nu) = \sigma(\nu).N \quad (2)$$

For absorption by a single vibration–rotation line the absorption cross-section is given by

$$\sigma(\nu) = S.g(\nu - \nu_0) \quad (3)$$

where  $S$  is the integrated linestrength in  $\text{cm.molecule}^{-1}$  and  $g(\nu - \nu_0)$  is the lineshape function in units of cm. The linestrength for a transition from lower state  $m$  to upper state  $n$  is given by<sup>1</sup>

$$S_{mn} = \left( \frac{C'v_{mn}}{Q_{\text{vib}}Q_{\text{rot}}} \right) \exp(-hc\nu_m/kT) [1 - \exp(-hc\nu_{mn}/kT)] |R_{mn}|^2 \quad (4)$$

where  $C'$  is a constant,  $v_{mn}$  is the transition wavenumber,  $Q_{\text{vib}}$  and  $Q_{\text{rot}}$  are the vibrational and rotational partition functions respectively,  $1 - \exp(-hc\nu_{mn}/kT)$  represents the effects of induced emission and must be considered for high temperatures and  $R_{mn}$  is the transition moment. The linestrength is independent of pressure and values are listed in databases such as HITRAN.<sup>14</sup> At high pressure where collisional broadening dominates, this is a Lorentzian function and at low pressures (less than a few torr), Doppler broadening dominates and the function is a Gaussian. At intermediate pressures a Voigt function is used which is a convolution of Lorentzian and Gaussian profiles. Numerical approaches to calculating the Voigt function have been described.<sup>15</sup>

The large increase in laser power with diode injection current makes it very difficult to measure small changes in absorption even using amplitude modulation as can be seen in Fig. 2. For enhanced sensitivity, harmonic detection is usually employed.

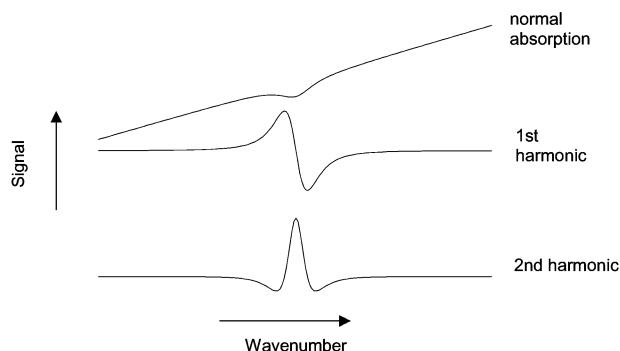


Fig. 2 (a) Direct or normal absorption. (The sloping background is due to the increase in laser power as the laser tunes across the absorption peak.) (b) First harmonic detection (1f). (c) Second harmonic detection (2f).

#### Absorption spectroscopy with harmonic detection techniques

There are several advantages of using harmonic detection where the laser wavelength is modulated at a frequency  $\omega$ . Firstly, it removes the sloping background, secondly, it can discriminate against features that do not show wavelength-dependent changes, and thirdly, it allows the signal to be detected at frequencies higher than the laser noise (1/f). As the laser frequency  $\nu_L$  is scanned across a single line absorption feature of line centre,  $\nu_0$ , the instantaneous laser frequency at time  $t$  is written

$$\nu(t) = \nu_L + \delta\nu \cos(\omega t) \quad (5)$$

where  $\delta\nu$  is the modulation amplitude. A dimensionless parameter  $m$  called the modulation coefficient is defined as  $m = \delta\nu/\gamma$  where  $\gamma$  is the half-width at half-maximum (HWHM) of the absorption line. The transmitted intensity can then be expressed as a cosine Fourier series:

$$I(\nu, t) = \sum_{n=0} H_n(\nu_L) \cos n\omega t \quad (6)$$

The Fourier coefficients are given by

$$H_n(\nu_L) = \frac{2}{\pi} \int_0^\pi I_0(\nu_L + m\gamma \cos\theta) \cdot \exp[-\sigma(\nu_L + m\gamma \cos\theta)NL] \cos n\theta d\theta \quad (7)$$

where  $\theta = \omega t$ . If there is no change in  $I_0$  as the absorption line is scanned then this equation becomes

$$H_n(\nu_L) = \frac{2I_0}{\pi} \int_0^\pi \exp[-\sigma(\nu_L + m\gamma \cos\theta)NL] \cos n\theta d\theta \quad (8)$$

Detection at the first harmonic ( $n = 1$ ), or 1f, with a phase sensitive detector or lock-in amplifier gives a first derivative-type lineshape (indeed it is proportional to the first-derivative when  $\gamma \gg \delta\nu$ ). Second harmonic detection ( $n = 2$ ), or 2f, is more generally used as it is most efficient at removing the sloping background without a large reduction in signal. Both first and second harmonic signals are also shown in Fig. 2. For  $n$ th harmonic detection, the effect of the residual amplitude modulation is to add terms proportional to  $H_{n+1}(\nu_L)$  and  $H_{n-1}(\nu_L)$  resulting in an asymmetric lineshape profile.

The maximum line centre 2f signal is obtained for a modulation coefficient,  $m$  of 2.2 In general the modulation

frequency is kept below 100 kHz and the technique is called wavelength modulation spectroscopy (WMS). The normal operating mode is then to scan the laser centre frequency  $\nu_L$  through the absorption line repetitively and to average the output signal from the lock-in amplifier.

Frequency modulation spectroscopy (FMS) has been successfully applied by several groups.<sup>6</sup> Here the modulation frequency is comparable to the absorption linewidth (several MHz to GHz) and the modulation produces sidebands on the laser centre frequency,  $\nu_L$ . The advantage is that detection occurs in low noise regions. An alternative is to use two closely spaced frequencies and detect at the difference frequency, selected to be of around 10–20 MHz. This is called two-tone frequency modulation spectroscopy (TTFMS). The relative merits of WMS, FMS and TTFMS have been discussed by several authors. Edwards and coworkers<sup>16</sup> achieved the largest signal to noise ratio of atmospheric water absorptions with TTFMS whereas Bomse and coworkers<sup>17</sup> considered WMS at high frequencies to be more sensitive although they used lead-salt lasers for their tests.

Typical spectrometer components for wavelength modulation spectroscopy are shown in Fig. 3. The diode laser is mounted on a thermoelectric heater and the temperature controlled to  $\pm 0.005$  °C to stabilise the emitted wavelength whilst the injection current is both ramped and modulated. The emitted beam is strongly divergent and is either collimated and employed in an open path arrangement or is directly coupled to a single mode fibre optic. The transmitted main beam is then sent to the measurement zone, which can be either an open path or closed cell arrangement and then detected by, typically, an InGaAs photodiode detector (PD) and preamplified. Beam splitters or fibre splitters are often used to pass a small percentage of the main beam through a reference gas cell which can be used for active locking of the emission wavelength. A third beam can then be used to measure the emitted laser power,  $I_0$ . Phase sensitive detectors (PSD) demodulate the signal and the output is sent to a computer for further processing and averaging. For higher sensitivity measurements the absorption path length can be increased by a multipass optical arrangement of either a White-type<sup>18</sup> or Herriott-type<sup>19</sup> for maximum beam coverage in a fixed volume of sample. Herriott cells have been more favoured for field measurements as the optical alignment is less critical than for White cells.

The minimum detectable absorbance is often limited by optical fringes caused by reflection off optical components resulting in an étalon effect. Typical absorbances of  $10^{-4}$ – $10^{-6}$  are readily detectable although  $10^{-7}$  is possible using frequency

modulation techniques and digital signal processing. Digital noise reduction schemes such as bandpass, Wiener, matched and Kalman filters have been described by Riris and coworkers.<sup>20</sup> Table 1 gives detection limits in the near infrared for several different gas species as a concentration  $\times$  pathlength (ppm.m) assuming a  $10^{-6}$  absorbance sensitivity with a signal to noise ratio of one in a 1 Hz bandwidth.

Instead of measuring the gas absorption directly it can be measured indirectly. Two such approaches that have recently been demonstrated with diode lasers are photoacoustic spectroscopy and cavity ring-down spectroscopy. In photoacoustic spectroscopy the absorption is detected as an acoustic wave with a microphone caused by the relaxation of the laser-excited molecules. Signals are enhanced by using resonant cells and it has already been demonstrated for field applications.<sup>21</sup> Cavity ring-down spectroscopy has the potential for even greater sensitivity.<sup>22</sup> A small fraction of the laser beam is coupled into an optical cavity and the time-decay of the light leaking out is measured. The decay or ring-down time depends on the presence of absorbing gas molecules and the effective path-lengths are several km leading to very high sensitivities. It is a promising technique but has yet to be demonstrated outside the research laboratory.

#### 4 Fundamental spectroscopy in the near infrared

Despite the narrow wavelength tuning range of NIR diode lasers they have been used for fundamental spectroscopic studies such as determination of line positions, temperature-dependent linewidths, pressure broadening parameters and improved electric dipole moment functions. The HITRAN database<sup>14</sup> is less comprehensive in the near-infrared region, especially for high temperature spectra yet molecular information in the NIR is crucial to understanding the chemical and physical behaviour of the media being investigated. This has been partly due to the lower priority for this type of information and to the increased complexity of overtone and combination bands due to perturbations in the spectra.

An example of this type of work is the spectral intensity and lineshape measurements in the first overtone band ( $\nu = 2-0$ ) of HF. The P(3) and P(6) transitions were measured with DFB lasers operating around 1.31 and 1.34  $\mu\text{m}$  respectively.<sup>23</sup> Lineshape measurements for HF pressures from 5 to 60 torr showed significant variation from the Voigt lineshape due to velocity-changing collisions that have the effect of reducing the

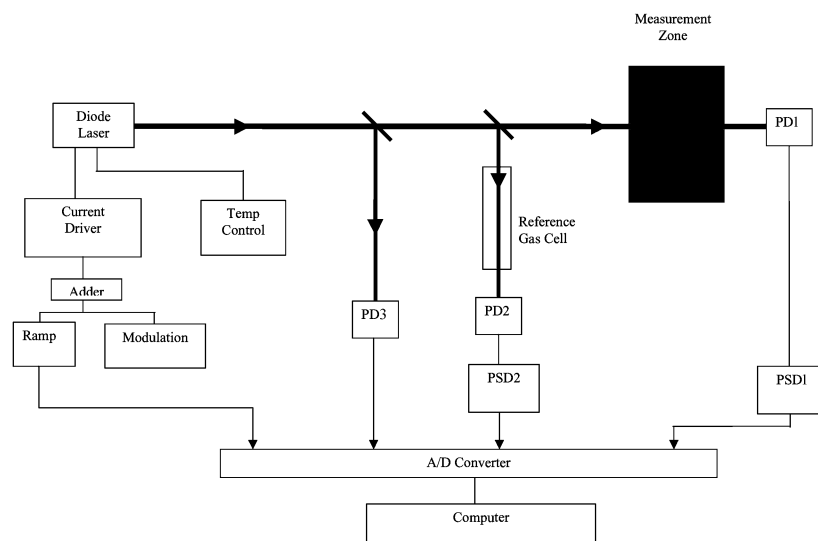


**Fig. 3** A typical near-infrared diode laser spectrometer arrangement for wavelength modulation spectroscopy. The optical beam is shown in bold. The measurement zone can be an open path through the atmosphere, or a reference gas cell, or a multipass absorption cell for example. PD is a photodiode detector/preamplifier and PSD is a phase sensitive detector.

**Table 1** Detection limits for several species as a concentration  $\times$  pathlength (ppm.m) assuming a  $10^{-6}$  absorbance sensitivity with a signal to noise ratio of one in a 1 Hz bandwidth.  $\gamma_L$  is the air-broadened half-width at 1 atm. Interference-free conditions are also assumed

	Wavenumber $\nu$ $\text{cm}^{-1}$	Wavelength $\lambda$ $\mu\text{m}$	Linestrength $S$ $\text{cm molecule}^{-1}$	Linewidth $\gamma_L$ $\text{cm}^{-1}$	Detection limits ppm.m
H <sub>2</sub> O	7327.692	1.365	$2.10 \times 10^{-20}$	0.095	0.006
	5413.911	1.847	$2.76 \times 10^{-20}$	0.095	0.004
HF	7823.821	1.278	$7.69 \times 10^{-20}$	0.033	0.001
HCl	5723.301	1.747	$1.18 \times 10^{-20}$	0.072	0.008
HBr	7458.082	1.341	$2.07 \times 10^{-23}$	0.080	5.0
HI	6489.026	1.541	$2.99 \times 10^{-22}$	0.050	0.2
H <sub>2</sub> S	6337	1.578	$1.30 \times 10^{-22}$	0.175	1.7
CH <sub>4</sub>	6046.965	1.654	$1.32 \times 10^{-21}$	0.050	0.05
CO	4288.290	2.332	$3.60 \times 10^{-21}$	0.060	0.021
	6377.407	1.568	$2.30 \times 10^{-23}$	0.060	3.261
CO <sub>2</sub>	4989.972	2.004	$1.33 \times 10^{-21}$	0.073	0.069
	6359.968	1.572	$1.85 \times 10^{-23}$	0.073	4.932
NO	3744.151	2.671	$1.04 \times 10^{-21}$	0.061	0.073
NO <sub>2</sub>	12500	0.800	$5.00 \times 10^{-23}$	0.073	1.825
N <sub>2</sub> O	4428.904	2.258	$1.22 \times 10^{-21}$	0.077	0.079
	5117.472	1.954	$5.11 \times 10^{-23}$	0.077	1.884
NH <sub>3</sub>	6478	1.544	$3.70 \times 10^{-22}$	0.060	0.203
O <sub>2</sub>	13142.58	0.761	$8.83 \times 10^{-24}$	0.050	7.078

Doppler component (Dicke narrowing). Improved lineshape fits were achieved with the Galatry (soft collision) and Rautian (hard collision) models both of which take this effect into account. The measured self-broadening coefficients varied considerably from those tabulated in HITRAN.

For high temperature measurements such as in combustion systems it is important to use an accurate value of the molecular partition function for determining the linestrength at temperatures other than the reference temperature. For example for methane the HITRAN database gives the molecular partition function as a third-order polynomial determined from best fit of the detailed summation over all energy levels. At 1000 K this underestimates the partition function approximated by a simple harmonic oscillator (SHO) model by around 40%. Nagali *et al.*<sup>24</sup> validated the partition function experimentally by measuring pure methane at pressures from 20 to 60 torr heated in a cell over a temperature range 400 to 915 K. The maximum variation between the measured strengths and the values calculated from the SHO model was <4% over this temperature range. A similar approach has been taken by Aizawa<sup>25</sup> for the OH radical measured around 1.55  $\mu\text{m}$ .

An example of NIR diode lasers being used for purely spectroscopic measurements is in the observation of the  $3\nu_2 \leftarrow 0$  overtone band of the molecular ion  $\text{H}_3^+$  using a 1.45  $\mu\text{m}$  InGaAsP diode laser by Oka and coworkers.<sup>26</sup> This study was motivated by the observation of the  $2\nu_2 \leftarrow 0$  overtone band in the Jovian atmosphere. The ions were generated in a low pressure AC discharge with either concentration or velocity modulation of the ions but with no laser modulation.

## 5 Applications

This section covers several recent application examples to illustrate the advantages of NIR diode laser spectroscopy. The first example of chemical vapour deposition reaction diagnostics illustrates *in situ* monitoring in a high temperature reactor at atmospheric pressure. The second example, illustrates rapid measurements in an open path arrangement. The third example describes remote measurements of the stratosphere with a balloon-borne NIR diode laser system. Finally, measurement of multiple parameters such as concentration, temperature and pressure through diode laser multiplexing is illustrated by reference to combustion diagnostics.

### (a) Chemical vapour deposition reaction diagnostics

Detecting species in hostile environments at high temperatures and high pressures is one of the capabilities of NIR diode laser spectroscopy. It has recently been demonstrated as an *in situ*, non-invasive probe of atmospheric pressure chemical vapour deposition (APCVD) processes and reactions, both for mechanistic studies and for process monitoring. APCVD is commonly used for depositing coatings or thin films onto substrates and the chemical mechanism is either primarily a gas phase chemical reaction or a surface chemical reaction. Invasive, *ex situ* techniques such as mass spectrometry and gas chromatography have been applied and although sensitive they can perturb the reaction being measured. For *in situ* measurements optical techniques offer the best approach. Broad-band near-infrared spectroscopy is now routinely used in process applications but the broad absorption peaks often require advanced chemometric analysis in order to extract useful information. Fluorescence approaches are limited by quenching effects at the pressures used in the reactors. FTIR spectroscopy has been the most successful and the complex spectra produced are perhaps most useful for the initial determination of species present. NIR diode laser spectroscopy can thus be considered to be complementary to FTIR spectroscopy. More sophisticated approaches such as the non-linear Raman technique CARS are more difficult to use but can supply point concentration information.<sup>27</sup>

An example of APCVD is the deposition of tin oxide on a glass substrate.<sup>28</sup> Tin oxide ( $\text{SnO}_2$ ) films are transparent and have low electrical resistivity. They have applications in solar cells, gas sensors and infrared reflectors for glass windows as they are mechanically very hard and able to withstand harsh environments. Several different precursors have been used for the generation of tin oxide films but in this case dimethyltin dichloride (DMT) was used with oxygen and water vapour. Thermal energy from the heated substrate (645 °C) initiated the gas phase reaction and the main products are hydrogen chloride and methane, although there are several additional products present in smaller amounts such as CO, CO<sub>2</sub>, CH<sub>3</sub>OH, CH<sub>2</sub>O, C<sub>2</sub>H<sub>2</sub>, C<sub>2</sub>H<sub>4</sub>, C<sub>2</sub>H<sub>6</sub>. Methane was monitored as a reaction product by detecting absorption of the first overtone of the C–H stretch,  $2\nu_3$ , with a band centre around 6004  $\text{cm}^{-1}$  (1665 nm) shown in Fig. 4. Linestrengths,  $S$ , in this band were of the order  $10^{-21}$   $\text{cm molecule}^{-1}$  which is approximately 100 times weaker than the  $\nu_3$  fundamental. The R(4) manifold around 6057.1  $\text{cm}^{-1}$  was selected as suitable for monitoring as it is a strong

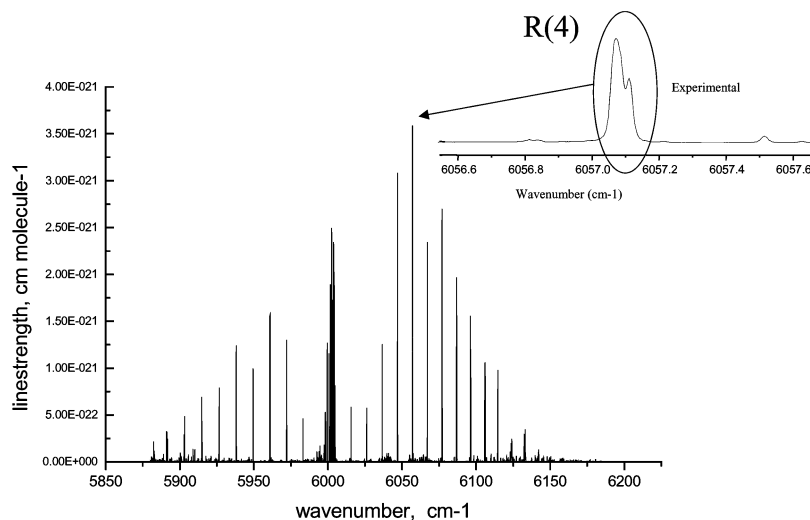


Fig. 4 The simulated  $2\nu_3$  band of methane around 1665 nm. Detail is shown of the R(4) manifold which was used for the CVD monitoring.

transition and there are no interferences from other species present. At atmospheric pressure, this criterion is more difficult to meet than at lower pressures due to the broader absorption peaks. In addition, at higher temperatures there are many more absorption lines as a result of the increased population of vibrational levels. This is especially true for water.

For rapid measurements, the modulated laser wavelength was set to the line centre absorption and stabilised by a 'first-derivative' line-locking technique.<sup>5</sup> A small fraction of the laser beam was sent through a reference gas cell and the first harmonic detected which gave a line centre output of zero volts. Drifts in the laser wavelength caused by temperature variations then produce offsets which send a compensating signal to the laser current driver either by direct analogue or digital means. Second-harmonic detection was then used for the sample beam.

The atmospheric pressure CVD reactors were of the cold-walled, horizontal flow design. The tin oxide film was deposited on a  $22.2 \times 9$  cm glass substrate maintained at a temperature of  $645^\circ\text{C}$  with a top glass plate about 10 mm above the substrate to ensure laminar flow. The NIR DFB diode laser beam was passed directly through the quartz glass walls of the reactor in an entirely non-invasive manner.

Fig. 5 shows the methane concentration profile during deposition. The precursors (DMT,  $\text{O}_2$  and  $\text{H}_2\text{O}$ ) are admitted at time (1) and the methane concentration rises to a maximum. The

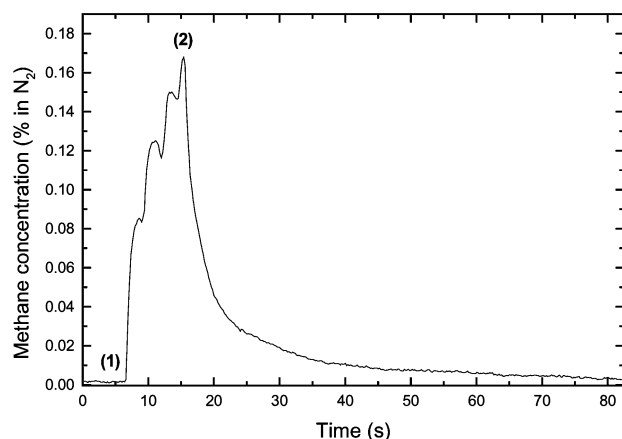


Fig. 5 Time evolution of methane in the APCVD reaction of dimethyltin dichloride, oxygen and water vapour to produce tin oxide on a glass substrate. Point (1) is the time that the precursors are admitted to the reactor and at time (2) the precursor flow is stopped and replaced by an equivalent flow of nitrogen. (Reprinted with permission from Wiley-VCH Verlag.)

undulations are caused by variations in the reaction rate due to the stepped nature of the water vapour inlet system. At time (2) the precursor flows are stopped and the methane is slowly removed from the reactor. By varying the precursor concentrations, different film thicknesses are produced. Plotting the peak methane concentration against the average film thickness after a fixed deposition time as in Fig. 6 shows that the two are

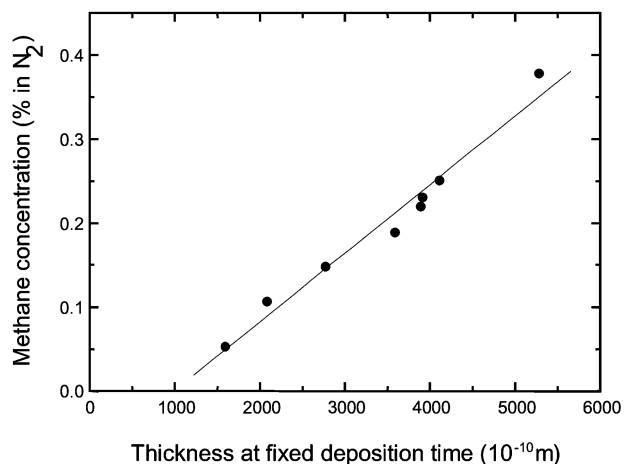


Fig. 6 Correlation of the peak methane concentration with tin oxide film thickness measured after the deposition. (Reprinted with permission from Wiley-VCH Verlag.)

directly correlated. The ratio of DMT to growth rate is different for each set of conditions whereas the ratio of methane concentration to the growth rate is constant. Determining methane concentration is therefore a more reliable measure of growth rate under varying reaction conditions.

The chemical kinetics of the reaction have been modelled using known rate constants for the elementary reactions. It is thought that methyl radical formation is promoted by water forming a complex with DMT which weakens the Sn- $\text{CH}_3$  bond. Combining the kinetics with computational fluid dynamics calculations allows methane concentrations to be calculated at each point in the reactor. Spatial measurements of methane with NIR diode laser spectroscopy have subsequently been carried out.

This application illustrates the many advantages of NIR diode laser absorption spectroscopy for rapid, *in situ* spatially resolved measurements in chemical process monitoring and control.

## (b) Remote vehicle emission environmental sensing

The principal molecular species emitted by car exhausts are water, carbon monoxide and dioxide, oxides of nitrogen, hydrocarbons and oxygenated hydrocarbons. The concentration of some of these species determines whether or not the vehicle is regarded as a polluting vehicle. One possible approach to the current worldwide urban air pollution problem is to identify which vehicles are polluting more than others and to remove them from the road. In order to do this with the minimum inconvenience to the remainder of the vehicle fleet requires a non-invasive and remote technique which is sufficiently sensitive and rapid to detect exhaust gases in moving vehicles.

Remote vehicle emission sensing was first developed by Stedman and coworkers at the University of Denver in the 1980's using broad-band infrared and ultraviolet spectroscopy to detect CO, CO<sub>2</sub>, hydrocarbons and NO.<sup>29</sup> This broad-band approach suffers from interferences mainly due to water vapour, is only capable of short pathlengths, and lacks sensitivity for certain gases. Mid-infrared diode laser spectroscopy has also been applied to the problem by Jimenez and coworkers.<sup>30</sup> They used two lead-salt diode lasers to measure absorptions in CO<sub>2</sub> at 2243 cm<sup>-1</sup> and NO around 1903 cm<sup>-1</sup> but the cryogenic cooling of the lasers and detectors makes the system unsuitable for prolonged field measurements. The Huddersfield group have applied near-infrared diode laser spectroscopy to the problem and have developed a sensor for the simultaneous detection of CO and CO<sub>2</sub>.<sup>31</sup> from vehicle exhausts.

One of the problems in determining the concentration (or mass emission rates) of exhaust gases in a remote manner is that it is very difficult to define the absorption pathlength. The exhaust plume spreads out on emission due to the effects of turbulence and diffusion and the probe beam will pass through different pathlengths of exhaust gas. The overlap will also be dependent on the height of the exhaust with respect to the probe beam. The usual approach is to measure the ratio of one gas, say CO, in relation to a constant tracer gas such as CO<sub>2</sub>. The ratio is then independent of the absorption pathlength. It is then possible to solve the combustion equations to determine an approximate concentration of CO.

In general it is necessary to employ a separate DFB diode laser for each gas to be monitored but fortuitously in the case of CO and CO<sub>2</sub> their overtone and combination bands overlap in the region around 1.5 μm although the linestrengths are very weak, of the order 10<sup>-23</sup> cm molecule<sup>-1</sup>.

Fig. 7 shows an example of suitable CO and CO<sub>2</sub> vibration-rotation lines for simultaneous detection within the narrow tuning range of the laser. Line-pair selection is important as both lines must be close enough together to fit the wavelength/current tuning range of the laser yet be far enough apart to be separately resolved. The selected lines must also be free from any other absorbing species such as water. This is a limitation of

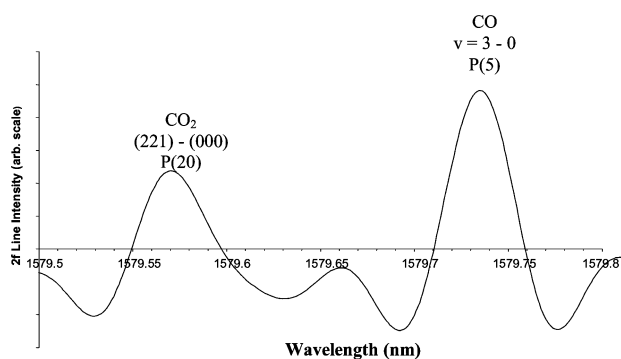


Fig. 7 Second harmonic spectrum of CO and CO<sub>2</sub> obtained from a car exhaust with the vehicle travelling at 40 km h<sup>-1</sup>. It has been background subtracted and an average of 5 scans taken at a rate of 12 Hz.

the broad-band approach. The HITRAN database<sup>14</sup> allows simulation of the spectral region and this can be verified by using an external cavity diode laser with a wide tuning range.

The Huddersfield sensor uses wavelength modulation and second harmonic detection with a 0.1 ms lock-in amplifier integration time. The line pair is scanned at a rate up to 100 Hz. Fig. 8 illustrates in schematic form the operation of the sensor.

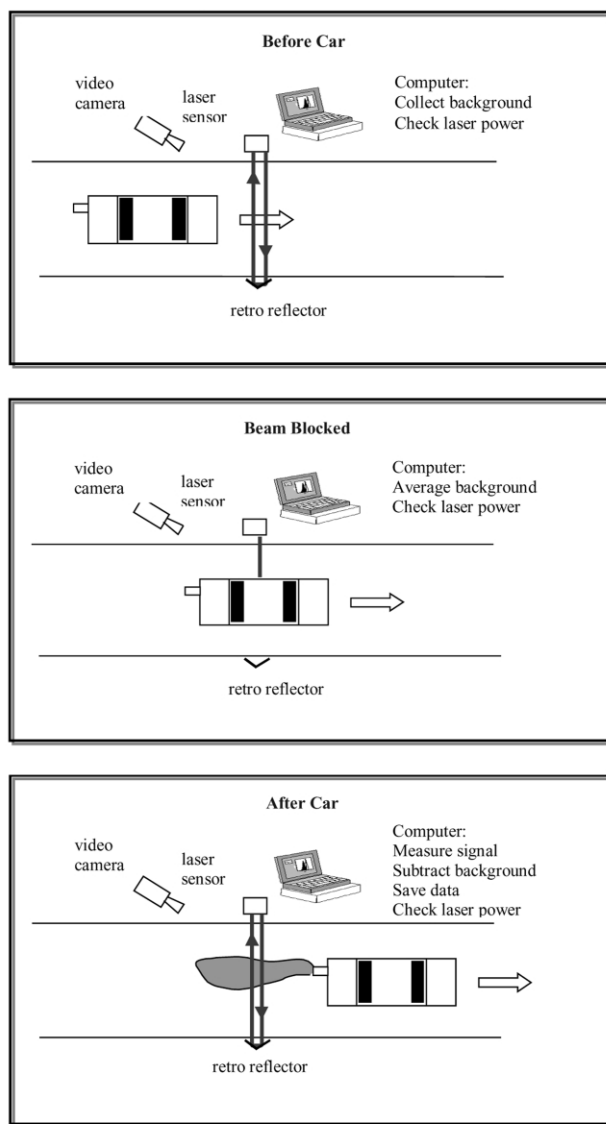


Fig. 8 Schematic of the operation of the near-infrared diode laser remote vehicle emission sensor.

The collimated laser beam is transmitted across the road to a retroreflector which returns the beam to the spectrometer for detection. Whilst there is no vehicle present the sensor continuously measures the background levels of CO and CO<sub>2</sub> (which can build up in street-canyons or tunnels). As a vehicle drives through the laser beam the controller averages the background concentration and awaits a measurement. When the return beam is received again CO/CO<sub>2</sub> scans are recorded and averaged for a period of up to 500 ms. The maximum absorptions occur at different times after the beam is returned due to the spatial arrangements of the exhaust pipe with respect to the probe beam. During the next 500 ms the spectra are processed and the background subtracted and a video or digital image of the vehicle is recorded. The maximum period between vehicles is 1 s allowing over 3600 vehicles to be screened in 1 h. The low power requirements of the diode laser sensor enable an unobtrusive rechargeable battery pack to be used without the need for noisy generators.

Fig. 7 illustrates the spectrum obtained of a car exhaust when the vehicle drives past at  $40 \text{ km h}^{-1}$  under normal operating conditions. It is an average of five spectra taken at a scan rate of  $12 \text{ Hz}$ . The  $\text{CO}_2$  absorption is P(20) from the (221)–(000) combination band at  $1579.574 \text{ nm}$  and the  $\text{CO}$  absorption is P(5) of the  $\nu = 3\text{--}0$  overtone band at  $1579.737 \text{ nm}$ .

There are many applications for NIR diode laser remote vehicle emission sensors. One is as a screening tool in a 'stop and check' arrangement for enforcement agencies such as the Vehicle Inspectorate in the UK. Another is to control low emission zones in town centres whereby a sensor is placed on each major road entering a town. The sensors could also be linked by optical fibres with a central control point housing the lasers.

Further work is being carried out to detect  $\text{NO}$  by its second overtone around  $1.8 \mu\text{m}$  and  $\text{NO}_2$  around  $0.68 \mu\text{m}$  by its electronic A–X transition. Hydrocarbons and benzene in particular can also be detected through their NIR spectra and opacity measurements at wavelengths where atmospheric gases do not absorb enable particulates to be detected. Several diode lasers are then easily multiplexed to send a single beam through the exhaust plume to detect multiple components after wavelength demultiplexing (see Section 5d).

NIR diode laser remote vehicle emission sensing illustrates the capabilities of rapid, non-invasive, interference free measurements of multicomponent gases.

### (c) Balloon-borne atmospheric monitoring

The high sensitivity and high spatial resolution possible with diode laser spectrometers makes them suitable for *in situ* atmospheric measurements of concentration profiles of species relevant to ozone depletion chemistry, the greenhouse effect and atmospheric chemistry in general. Spectrometers have been mounted on balloons, aircraft and even rockets. Lead-salt diode lasers have been used by Webster's group at JPL most recently for the determination of the long lived tracers  $\text{N}_2\text{O}$  and  $\text{CH}_4$ , the shorter-lived tracer  $\text{CO}$  and the chemically reactive species  $\text{HCl}$  and  $\text{NO}_2$  in the balloon-borne ALIAS II instrument.<sup>32</sup> Durry and Megie of CNRS<sup>33</sup> have developed a balloon-borne near-infrared diode laser spectrometer called SDLA (Spectromètre à Diode Laser Accordables) for *in situ* measurement of  $\text{CH}_4$  and  $\text{H}_2\text{O}$  in the altitude range 1 to 31 km.

There are three main reasons for measuring methane. Firstly, methane is a greenhouse gas, secondly it is involved in ozone chemistry by reducing  $\text{Cl}$  to the reservoir species  $\text{HCl}$  ( $\text{CH}_4 + \text{Cl} \rightarrow \text{HCl} + \text{CH}_3$ ) and thirdly, as a long-lived tracer it can be used to give information on air-mass transport.

An open path multipass Herriott cell giving a 56 m optical path length is the main part of the gondola (Fig. 9). Two separate single mode fibre-coupled diode laser beams are fed into the cell by means of a small Cassegrain-type telescope. The optical paths are different and the beams are sent to two detectors. For methane the R(3) vibration–rotation line at  $6046.9 \text{ cm}^{-1}$  ( $1.653 \mu\text{m}$ ) of the  $2\nu_3$  band was detected. For water, the P(3) line at  $7181.17 \text{ cm}^{-1}$  of the  $\nu_1 + \nu_3$  combination line was used. Instead of harmonic detection, a differential approach was employed to allow precise determination of the zero absorption baseline and to give access to the full molecular lineshape. On each channel a small fraction of the beam was detected before it entered the Herriott cell to provide a background signal. A differential analogue amplifier then subtracts this background from the signal derived from the cell. In addition a reference channel was also recorded containing a low pressure reference gas cell. Four spectra are recorded for each gas along with the local pressure, temperature and GPS information and the data is saved for post-flight processing.

Fig. 10 (a) shows molecular absorption  $A(\sigma)$  of methane as a function of altitude for a recent test flight. The balloon was

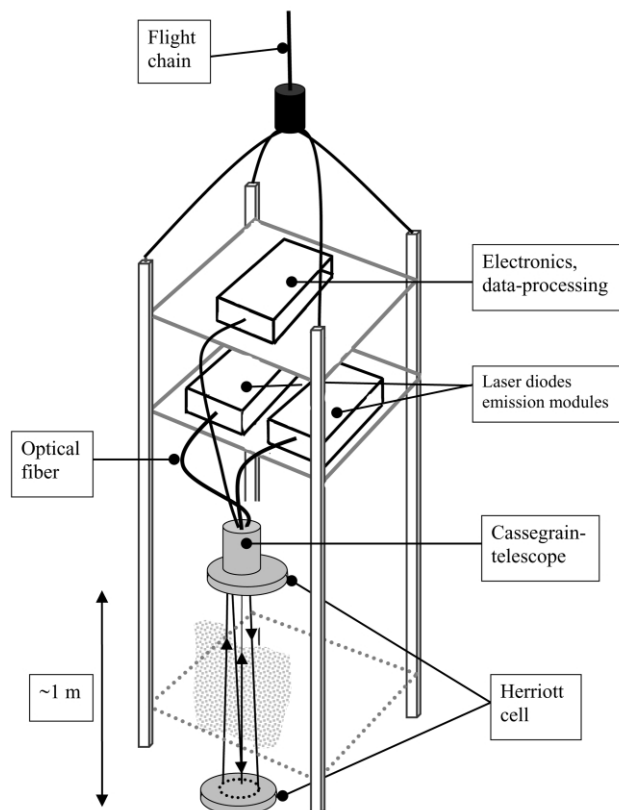


Fig. 9 Schematic of the SDLA gondola showing the open path Herriott cell with a 56 m pathlength. Single mode optical fibres transmit the two diode laser beams to the cell. The height of the instrument is approximately 3 m and the weight about 100 kg. (Reprinted with permission from Optical Society of America.)

inflated with  $35,000 \text{ m}^3$  of hydrogen to give a float altitude of around 30.5 km. A slow descent down to around 14 km lasted 3.5 h. The absorption depth decreases from 0.32% at 1.4 km to 0.025% at 30.6 km and the lineshape becomes more Doppler-limited. The maximum occurs at around 12 km due to the reduction of collisional effects. Fig. 10 (b) shows the methane vertical profile in the Arctic vortex above Kiruna (Sweden) in February 1999. The error in the derived methane mixing ratio was determined to be 5% which increased to 10% for altitudes above 25 km.

This example demonstrates the capability of fibre-coupled NIR DFB diode lasers for atmospheric measurements in the stratosphere with severe temperature gradients even using direct absorption techniques rather than harmonic detection methods.

### (d) Combustion diagnostics

Diode laser techniques provide fast, sensitive and non-intrusive means of measuring several quantities simultaneously in gas flows such as combustion systems. For example, gas density and pressure from the absorption, temperature from the intensity ratio of two adjacent lines and gas velocity from Doppler shift measurements of the absorption lines. Diode laser sensors have the potential to be both a diagnostic tool and also act as part of an active control strategy. Hanson's group at Stanford have made many important contributions in this area, for example.<sup>34</sup>

**Temperature measurements.** Although there is a temperature dependence on the lineshapes of individual transitions it is more sensitive to determine temperature by taking the ratio



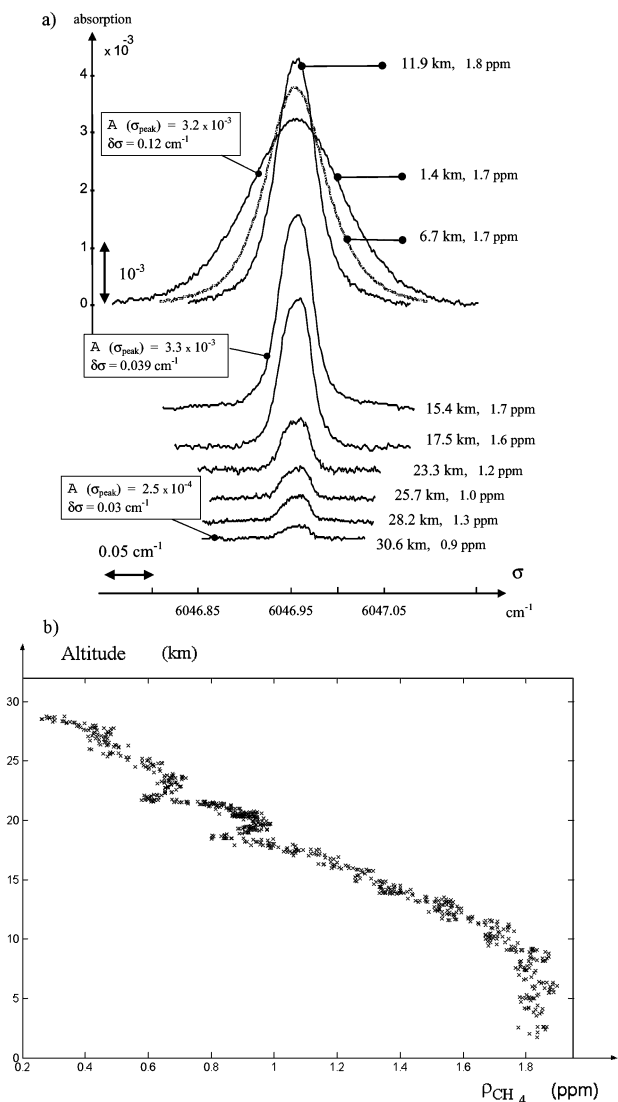


**Fig. 10** (a) Molecular absorption as a function of altitude for the R(3) line of the  $2\nu_3$  band of methane at  $6046.95\text{ cm}^{-1}$  obtained during a test flight of the SDLA. Further details are given in the text. (b) Vertical methane concentration profile obtained during the flight of the SDLA in the Arctic vortex from Kiruna in Sweden in 1999. (Reprinted with permission from Optical Society of America.)

of two absorption line intensities. This ratio can be expressed as:

$$R = \frac{S_1(T_0) \cdot g(\nu - \nu_1)}{S_2(T_0) \cdot g(\nu - \nu_2)} \exp \left[ - \left( \frac{hc}{k} \right) (E_1'' - E_2'') \left( \frac{1}{T} - \frac{1}{T_0} \right) \right] \quad (9)$$

where  $S_i(T_0)$  is the line strength of transition  $i$  at a reference temperature  $T_0$ ,  $g(\nu - \nu_i)$  is the normalised lineshape function,  $E''_i$  is the lower state energy level and  $T$  is the temperature to be measured. So, for a given pair of lines, the intensity ratio is a function of temperature only. The sensitivity of this ratio to temperature very much depends on selecting transitions with an appropriate difference in their lower state energy levels ( $E''_1 - E''_2$ ). The Huddersfield group have used overtone and hot band lines from carbon monoxide for probing combustion systems e.g. P(9) from  $\nu = 3-0$  and R(12) from  $\nu = 4-1$  measured using a single sweep of a DFB laser. For  $\text{H}_2\text{O}$ , Hanson and coworkers used two DFB lasers to monitor transitions near  $1343\text{ nm}$  ( $\nu_1 + \nu_3$ ) and  $1392\text{ nm}$  ( $2\nu_1$ ). When the temperature is known the concentration or mole fraction can be determined. With a single laser operating around  $7212\text{ cm}^{-1}$  the  $\text{H}_2\text{O}$  line pair  $6_{43} \leftarrow 6_{42}$  and  $3_{13} \leftarrow 3_{12}$  could be measured.<sup>35</sup> The sensitivity of the intensity ratio to temperature is shown in Fig. 11. At  $400\text{ K}$  a measurement error in  $R$  of  $0.01$  corresponds to an error of  $1.8\text{ K}$

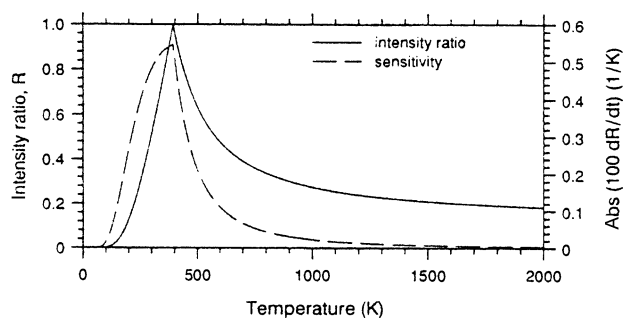


**Fig. 11** Intensity ratio and its sensitivity to temperature *versus* temperature for the water line pair  $6_{43} \leftarrow 6_{42}$ ,  $3_{13} \leftarrow 3_{12}$  around  $7212.9\text{ cm}^{-1}$ . The intensity ratio is defined so that it is always less than unity. (Reprinted with permission from Optical Society of America.)

in temperature but at  $1350\text{ K}$  with the same measurement precision the error increases to  $100\text{ K}$ .

**Multiple parameters.** In experiments in a shock tube ( $\text{H}_2\text{O}$  and  $\text{O}_2$ ) the diode laser beam was split into four: one passed through the shock tube at  $90^\circ$  to the shock front, one passed at  $60^\circ$ , one beam measured the laser intensity and the final beam passed through an étalon to measure the wavelength tuning rate. Direct absorption measurements were made at high repetition rates of  $10\text{ kHz}$ . The gas velocity could be extracted from the frequency shift of the  $\text{H}_2\text{O}$  absorptions due to the Doppler effect. An iterative fit using Voigt profiles was then used to determine temperature from the intensity ratio and then pressure/concentration from the fractional absorbance which was in the range  $3\text{--}30\%$ . Gas velocity was measured in the range  $300\text{ to }1700\text{ m s}^{-1}$ , temperature in the range  $460\text{ to }1700\text{ K}$  and pressure from  $0.02\text{ to }1.1\text{ atm}$ . From these results density and mass and momentum fluxes could also be extracted. Fig. 12 shows the type of raw spectra obtained in these shock tube experiments.

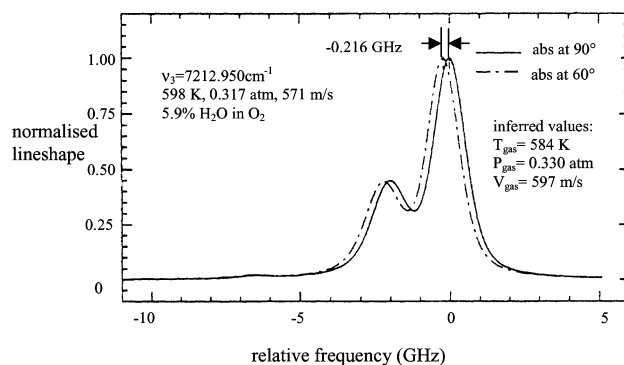


**Fig. 12** Absorption lineshapes of  $\text{H}_2\text{O}$  from the shock tube experiments described in the text. The  $3_{13} \leftarrow 3_{12}$  line is located  $-2.04\text{ GHz}$  from the larger  $6_{43} \leftarrow 6_{42}$  line at  $7212.950\text{ cm}^{-1}$ . The inferred gas velocity, temperatures and pressures are  $597\text{ m s}^{-1}$ ,  $588\text{ K}$  ( $60^\circ$ ),  $580\text{ K}$  ( $90^\circ$ ),  $0.332\text{ atm}$  ( $60^\circ$ ), and  $0.328\text{ atm}$  ( $90^\circ$ ), respectively. (Reprinted with permission from Optical Society of America.)

For the measurement of multicomponents and multiparameters several diode laser spectrometers are required simultaneously. Fortunately, multiplexing the lasers is straightforward with the use of optical fibres. Wavelength division multiplexing or time-domain multiplexing techniques have been developed and an example of such a configuration is shown in Fig. 13. Here, four different lasers are used for the simultaneous determination of  $\text{H}_2\text{O}$  mole fraction, temperature and pressure. Three lasers probe  $\text{H}_2\text{O}$  transitions and a fourth measures the zero absorption intensity which is necessary because line-broadening effects preclude the baseline being measured by scanning across the vibration-rotational peaks of  $\text{H}_2\text{O}$ . The four wavelengths are combined and transmitted by a single fibre

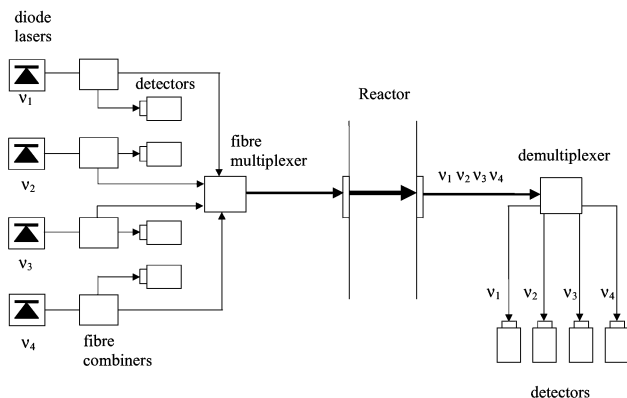


**Fig. 13** Schematic of a 4-laser wavelength-multiplexing arrangement. Each laser wavelength is passed down a single fibre optic and then transmitted across the measurement zone. After collection of the transmitted beam the wavelengths are demultiplexed and detected separately.

optic to the measurement region. After transmission, the combined beam is demultiplexed by, for example, a grating.

## 6 Conclusions and future prospects

In this review we have attempted to highlight the new laser sources and techniques in NIR diode laser spectroscopy that are now being applied to a wide range of different environments. Several applications have been described here in more detail to illustrate the capabilities of rapid, non-invasive measurements with high selectivity. Many other application areas in chemistry, physics, materials science and even medical monitoring through diode laser breath testing are becoming apparent. It has also been shown that use of wavelength multiplexing bridges the gap between FTIR and single diode laser spectroscopy. New laser sources such as antimonide diode lasers and quantum cascade lasers continue to be developed which will take many of the advantages of NIR diode laser spectroscopy into the longer wavelength and thus higher intensity regions. Higher sensitivities can also be attained by combining diode lasers with cavity ring down spectroscopy but it remains to be seen whether this can successfully be applied in the field. Finally, the potential for micro-sensors perhaps through intracavity absorption methods may lead to an even wider distribution of diode laser gas sensors.

## 7 Acknowledgements

The author would like to thank the graduate students of the Huddersfield group, Robert Holdsworth, Simon Barrass and Yvan Gérard whose work has contributed to some of the experiments described here. Thanks are also given to the University of Huddersfield and the European Union for financial support.

## 8 References

- 1 C. R. Webster, R. J. Menzies and E. D. Hinkley, in *Laser Remote Chemical Analysis*, ed. R. M. Measures, Wiley, New York, 1988.
- 2 D. J. Brassington, in *Spectroscopy in Environmental Science*, ed. R. J. H. Clark and R. E. Hester, Wiley, New York, 1995.
- 3 U. Platt, in *Air Monitoring by Spectroscopic Techniques*, ed. M. W. Sigrist, Wiley, New York, 1994.
- 4 S. Svanberg, in *Air Monitoring by Spectroscopic Techniques*, ed. M. W. Sigrist, Wiley, New York, 1994.
- 5 M. Fehér and P. A. Martin, *Spectrochim. Acta A*, 1995, **51**, 1579.
- 6 P. Werle, *Spectrochim. Acta A*, 1998, **54**, 197.
- 7 J. Hecht, *The Laser Guidebook*, 2nd edn., McGraw-Hill, New York, 1992.
- 8 A. R. Adams, C. T. Elliott, A. Krier and B. N. Murdin, *Philos. Trans. R. Soc. London, Ser. A*, 2001, **359**, 455.
- 9 Y. Rouillard, F. Genty, A. Perona, A. Vicet, D. A. Yarekha, G. Boissier, P. Grech, A. N. Baranov and C. Alibert, *Philos. Trans. R. Soc. London, Ser. A*, 2001, **359**, 581.
- 10 M. Tacke, *Philos. Trans. R. Soc. London, Ser. A*, 2001, **359**, 547.
- 11 H. P. Zappe, M. Hess, M. Moser, R. Hoevel, K. Gulden, H. P. Gauggel and F. diSopra, *Appl. Opt.*, 2000, **39**, 2475.
- 12 J. Faist, F. Capasso, D. L. Sivco, C. Sirtori, A. L. Hutchinson and A. Y. Cho, *Science*, 1994, **264**, 553.
- 13 C. Sirtori, H. Page and C. Becker, *Philos. Trans. R. Soc. London, Ser. A*, 2001, **359**, 505–522.
- 14 L. S. Rothman, C. P. Rinsland, A. Goldman, S. T. Massie, D. P. Edwards, J.-M. Flaud, A. Perrin, C. Camy-Peyret, V. Dana, J.-Y. Mandin, J. Schroeder, A. McCann, R. R. Gamache, R. B. Wattson, K. Yoshino, K. V. Chance, K. W. Jucks, L. R. Brown, V. Nemtchinov and P. Varanasi, *J. Quant. Spectrosc. Radiat. Trans.*, 1998, **60**, 665.
- 15 J. Humlicek, *J. Quant. Spectrosc. Radiat. Trans.*, 1979, **21**, 309.
- 16 C. S. Edwards, G. P. Barwood, P. Gill, B. Schimer, H. Venzke and A. Melling, *Appl. Opt.*, 1999, **38**, 4699.
- 17 D. S. Bomse, A. C. Stanton and J. A. Silver, *Appl. Opt.*, 1992, **31**, 718.
- 18 J. U. White, *J. Opt. Soc. Am.*, 1942, **32**, 285.
- 19 D. R. Herriott, H. Kogelnik and R. Kompfner, *Appl. Opt.*, 1964, **3**, 523.
- 20 H. Iiris, C. B. Carlisle, R. E. Warren, D. E. Cooper, R. U. Martinelli, R. J. Menna, P. K. York, D. Z. Garbuzov, H. Lee, J. H. Abeles, N. Morris, J. C. Connolly and S. Y. Narayan, *Spectrochim. Acta A*, 1996, **52**, 843.
- 21 M. Fehér, Y. Jiang, J. P. Maier and A. Miklós, *Appl. Opt.*, 1993, **33**, 1655.
- 22 Y. He, M. Hippler and M. Quack, *Chem. Phys. Lett.*, 1998, **289**, 527.
- 23 S. I. Chou, D. S. Baer and R. K. Hanson, *J. Mol. Spectrosc.*, 1999, **195**, 123.
- 24 V. Nagali, S. I. Chou, D. S. Baer, R. K. Hanson and J. Segall, *Appl. Opt.*, 1996, **35**, 4026.
- 25 T. Aizawa, *Appl. Opt.*, 2001, **40**, 4894.
- 26 S. S. Lee, B. F. Ventrudo, D. T. Cassidy, T. Oka, S. Miller and J. Tennyson, *J. Mol. Spectrosc.*, 1991, **145**, 222.
- 27 M. J. Davis and M. E. Pemble, *J. Phys. IV*, 1999, **9**, 8.
- 28 R. J. Holdsworth, P. A. Martin, D. Raisbeck, J. Rivero, H. E. Sanders, D. Sheel and M. E. Pemble, *Chem. Vap. Dep.*, 2001, **7**, 39.
- 29 G. A. Bishop and D. H. Stedman, *Acc. Chem. Res.*, 1996, **29**, 489.
- 30 J. L. Jimenez, M. D. Koplow, D. D. Nelson, M. S. Zahniser and S. E. Schmidt, *J. Air Waste Man. Assoc.*, 1999, **49**, 463.
- 31 S. Barrass, R. J. Holdsworth, Y. Gerard and P. A. Martin, *The Third International Conference on Urban Air Quality*, Paper RS 2.1, 19–23 March 2001, Loutraki, Greece.
- 32 D. C. Scott, R. L. Herman, C. R. Webster, R. D. May, G. J. Flesch and E. J. Moyer, *Appl. Opt.*, 1999, **38**, 4609.
- 33 G. Durry and G. Megie, *Appl. Opt.*, 1999, **38**, 7342.
- 34 V. Nagali and R. K. Hanson, *Appl. Opt.*, 1997, **36**, 9518.
- 35 M. P. Arroyo, S. Langlois and R. K. Hanson, *Appl. Opt.*, 1994, **33**, 3296.